Degradation of Organic Dyes via Bismuth Silver Oxide Initiated Direct Oxidation Coupled with Sodium Bismuthate Based Visible Light Photocatalysis

ARTICLE *in* ENVIRONMENTAL SCIENCE & TECHNOLOGY · MAY 2012

Impact Factor: 5.33 · DOI: 10.1021/es3001954 · Source: PubMed

7 AUTHORS, INCLUDING:

Kai Yu
Michigan State University
9 PUBLICATIONS **274** CITATIONS
SEE PROFILE

Cun Liu
Michigan State University
10 PUBLICATIONS **153** CITATIONS
SEE PROFILE

Hui Li
Michigan State University
150 PUBLICATIONS **2,202** CITATIONS
SEE PROFILE

Cheng Sun
Nanjing University
180 PUBLICATIONS **3,212** CITATIONS
SEE PROFILE

Environmental Science & Technology

Article

pubs.acs.org/est

Degradation of Organic Dyes via Bismuth Silver Oxide Initiated Direct Oxidation Coupled with Sodium Bismuthate Based Visible Light Photocatalysis

Kai Yu,[†,‡,§] Shaogui Yang,[†] Cun Liu,[‡] Hongzhe Chen,[†] Hui Li,[‡] Cheng Sun,*[,†] and Stephen A. Boyd*[,‡]

[†]State Key Laboratory of Pollution Control and Resource Reuse, School of the Environment, Nanjing University, Nanjing 210093, P.R. China

[‡]Department of Crop and Soil Sciences, Michigan State University, East Lansing, Michigan 48824, United States

[§]Institute of Wastes and Soil Environment, Shanghai Academy of Environmental Sciences, Shanghai 200233, P.R. China

Supporting Information

ABSTRACT: Organic dye degradation was achieved via direct oxidation by bismuth silver oxide coupled with visible light photocatalysis by sodium bismuthate. Crystal violet dye decomposition by each reagent proceeded via two distinct pathways, each involving different active oxygen species. A comparison of each treatment method alone and in combination demonstrated that using the combined methods in sequence achieved a higher degree of degradation, and especially mineralization, than that obtained using either method alone. In the combined process direct oxidation acts as a pretreatment to rapidly bleach the dye solution which substantially facilitates subsequent visible light photocatalytic processes. The integrated sequential direct oxidation and visible light photocatalysis are complementary manifesting a > 100% increase in TOC removal, compared to either isolated method. The combined process is proposed as a novel and effective technology based on one primary material, sodium bismuthate, for treating wastewaters contaminated by high concentrations of organic dyes.

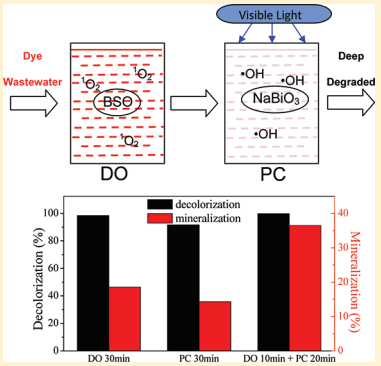

INTRODUCTION

Modern commercial dyes are characterized by strong structural and color stability imparted by their high degree of aromaticity and extensively conjugated chromophores. The production and widespread use of dyes inevitably results in their unintended release into the environment where they pose potential threats to human and ecological health. A common example is the release of polluted effluents generated from the production and use of dyes into surface waters. Industrial dyeing processes lead to the annual discharge of 30 000−150 000 tons of dyes into receiving waters.[1] The severely affected water presents not only adverse aesthetic coloration but also contains significant amounts of carcinogenic and mutagenic organic substances.[2,3]

Conventional wastewater treatment technologies are ineffective for removing dyes because many dye compounds are highly resistant to biological, physical, or chemical treatments.[1] Therefore, considerable effort has been made to develop advanced methods for remediating dye-contaminated waters. Among the treatment methods employed, photocatalytic technologies are widely applied due to their potential capability for complete degradation of organic dye molecules to mineralized end products such as CO_2 and NH_3.[4] The capacity for mineralization originates from •OH radicals (oxidation potential is 2.8 V) generated in photocatalytic processes, which render many complex organic compounds susceptible to decomposition.[2] Visible light photocatalysis has attracted growing attention as one type of photocatalysis.[5] The most significant advantage is it can be driven by visible light (43% of the solar spectrum) rather than UV light (5% of the solar spectrum) which is the only energy source utilized in traditional photocatalysis.[5] Efficiently utilizing inexpensive and inexhaustible solar energy while preserving most of the merits of traditional photocatalysis endues it with great promise for wastewater purification.

To improve treatment efficacy of photocatalysis, it is sometimes used in combination with other dye wastewater treatment techniques such as sonolysis and membrane filtration.[3,6−8] Although such combinations may lead to improved decolorization and mineralization, the attendant drawbacks of these ancillary techniques, e.g. prolonged treatment times, increased external energy inputs, and expensive equipment, have hindered their implementation. Most previous work aimed at improving this visible light photocatalysis has been devoted to developing improved photocatalysts.[9,10] The intensity of solar irradiation is not adjustable, and this is an inherent limitation of visible light photocatalysis for contaminant degradation that cannot be fundamentally ameliorated by developing high activity catalysts. This limitation is especially problematic for the decontamina-

Received: January 17, 2012
Revised: May 10, 2012
Accepted: May 22, 2012
Published: May 22, 2012

tion of highly concentrated, dark-colored, dye-contaminated wastewaters.[6] Therefore, to fully harness the important advantages of visible light photocatalytic treatment of dye-contaminated wastewaters, new methods are needed that effectively achieve color removal.

Perovskite-type metal oxides are known for their narrow band gap and high photocatalytic activity, and hence have become prominent in the field of visible light photocatalysis.[11,12] One newly developed member of the perovskite family, $NaBiO_3$, has photocatalytic activity against a broad range of pollutants such as phenol, PAHs, and dyes; these compounds are extensively degraded by $NaBiO_3$ in the presence of visible light irradiation.[13−15] Based on the previous characterization results,[13−17] the high photocatalytic performance of $NaBiO_3$ is ascribed to the rapid mobility of photo-generated electrons and strong visible light absorption ability. Perovskite-like metal oxides have also been reported to possess oxygen storage capacity that can be successfully utilized for direct oxidation of environmental contaminants.[18,19] Recently, we reported a direct oxidation method that utilized $NaBiO_3$-based bismuth silver oxide (BSO) to rapidly degrade organic dyes in aqueous medium with simple stirring.[20] No external energy source or irradiation was required for the reaction to proceed. An advantage of the oxidative technique is that BSO can be used to degrade sequential additions of dye without significant fouling or loss of activity. The characterization of BSO and its corrosion products revealed that Ag species were reduced to metallic silver, Bi(V) in BSO wa progressively reduced, and BSO was transformed into the $Bi_2O_2CO_3$ during the reaction process. BSO functioned predominantly as an oxidant in the direct oxidative reactions. Singlet oxygen ($^1O_2$) was identified as the major reactive species generated by BSO for the degradation of dyes. However, degradation was incomplete, especially with respect to the degree of dye mineralization achieved in aqueous solution. The central objective of this study was to evaluate a $NaBiO_3$ based dye treatment method that combines direct noncatalytic oxidation (DO) and visible light photocatalysis (PC) to achieve rapid decolorization and mineralization of dye-contaminated wastewater, especially highly concentrated dye solutions that would not be amenable to conventional visible light photocatalytic-based technologies. To advance mechanistic understanding of these processes, a related objective was to elucidate the generation, identity, and role of active oxygen species involved in dye degradation. Crystal violet (CV) (Figure S1) is a typical triphenylmethane dye containing six *N*-methyl groups at either side of the benzene ring. It has been reported to be toxic to mammalian cells, and is a mutagen as well as a mitotic poison.[21]

EXPERIMENTAL SECTION

Chemicals and Materials. $NaBiO_3{\cdot}2H_2O$ (>80%) was purchased from LI-DE Offset Chemical Material Co. Ltd. Crystal violet (CV) was obtained from Fluka. 5,5-Dimethyl-1-pyrroline-*N*-oxide (DMPO) spin-trap reagent and 99% *N*,*O*-bis-(trimethylsilyl)-trifluoroacetamide with 1% trimethylchlorosilane (BSTFA/TMCS) were supplied by Sigma-Aldrich. All other dyes and silver nitrate were purchased from Sinopharm Chemical Reagent Co.

Combined Process of Direct Oxidation and Visible Light Photocatalysis. Generally, the combined process was simply conducted by integrated sequential direct oxidation and visible light photocatalysis stage in which each stage was given appropriate reaction time in order to maximize the overall performance. The typical experimental procedures of each reaction stage adopted for combined process to degrade dye are described below.

Direct Oxidation (DO). The BSO was prepared by adding 0.2 g of $NaBiO_3{\cdot}2H_2O$ to 100 mL of $AgNO_3$ solution (containing 0.1 g $AgNO_3$) with stirring. After ∼1 min, the resulting black BSO solid was separated by centrifugation, washed with deionized water, then added to an aluminum-foil-wrapped 150-mL flask which functioned as a reactor to conduct the DO experiments. Then dye solutions (100 mL) at various concentrations were added to the flask, and the suspension was stirred at constant speed throughout the degradation reaction process using a magnetic stir plate and bar. Additional details of the DO procedure can be found in Yu et al.[20] Typically in the combined process (described below), the DO stage ran without interruption until the dye solution was extensively decolorized.

Visible Light Photocatalysis (PC). Before initiating the photocatalytic process, BSO particles in the DO reactor effluent were removed by centrifugation at 8000 rpm for 2 min, then the supernatant was immediately transferred to the photocatalytic chamber. The PC degradation experiments were performed in a custom-built chamber as reported previously.[13] A 750-W xenon lamp (Shanghai Hua Lun Lamp Factory, China) embedded in a cylindrical circulating water jacket (quartz) was positioned above the 150-mL photocatalytic reactor. The reactor was covered with a 400-nm cutoff filter (Beijing HZXD Optics Technology Co. Ltd., China) and wrapped with aluminum foil to ensure illumination by visible light only. A magnetic stirrer was placed under the reactor, and a stir bar was used to ensure maximum contact between the reaction solution and photocatalyst. A 55-W fan was used to keep the chamber at ambient temperature. After supernatant from the DO treatment was transferred into the reactor, 0.2 g of $NaBiO_3{\cdot}2H_2O$ (photocatalyst) was added to initiate photocatalytic treatment. Preliminary experiments confirmed that adsorption of dyes used in this study and their degradation intermediates, on the BSO particles or $NaBiO_3{\cdot}2H_2O$ photocatalyst surface, was insignificant and they were stable under visible light irradiation only. For comparison, the DO and PC reactions were employed separately to treat the dye solutions utilizing otherwise identical reaction conditions.

Analytical Procedures. For both processes, portions of aqueous suspensions or solutions were sampled (2 mL) at predetermined intervals, placed into centrifuge tubes, and centrifuged at 12 000 rpm for 2 min. Dye concentrations in these samples were measured using a Shimadzu UV-2450 spectrophotometer at the corresponding absorbance maximum of the dye. Total organic carbon (TOC) content of the supernatants were measured using a Shimadzu carbon analyzer (model TOC-5000A). A liquid chromatography-electrospray ionization tandem mass spectrometer (LC/MS/MS) (Thermo) equipped with a C18 inversed-phase column (150 mm × 4.6 mm i.d., Phenomenex) was utilized to identify CV degradation products. Aqueous samples obtained as described above were injected into the LC/MS/MS system. The mobile phase was acetonitrile/water (68:32, v/v) at a flow rate of 0.2 mL/min, and MS detection was performed in positive mode with a full scan mass spectrum over the m/z range 50−500. Degradation products (nonmineralized) were further identified by gas chromatography/mass spectrometry (GC/MS) analysis using a Thermo Finnigan gas chromatograph interfaced with a Polaris Q ion trap mass spectrometer and with a DB-5 GC column (30 m × 0.25 mm i.d., 0.25 μm, Agilent). The oven temperature

dx.doi.org/10.1021/es3001954 | Environ. Sci. Technol. 2012, 46, 7318−7326

program was set from 60 °C (2 min) to 110 at 7 °C min^{-1} and from 110 to 300 °C (8 min) at 13 °C min^{-1}. The MS was operated in positive electron impact (EI) ionization mode with electron energy of 70 eV. The injector temperature was 240 °C. Helium was used as carrier gas. Prior to GC/MS analysis, samples (15 mL) were obtained as described above then placed in a 40-mL glass tube. The pH was adjusted to ~2.5 using 0.5 M HCl, then the CV reaction solution was extracted with 5 mL of dichloromethane three times. The combined extracts were rotary evaporated (50 °C) in a pyriform flask to 1 mL, and then transferred into a 2-mL vial and blow-dried using a gentle stream of N_2 blow drying. To methylate the reaction byproducts, 0.2 mL of BSTFA/TMCS was added into the vial and mixed with the residue at 50 °C for 30 min. The DMPO trapping experiment was carried out under oxygen-free conditions to avoid any interference due to the quenching effect of molecular oxygen. The radical adduct of DMPO was prepared by sampling the reaction solution with a syringe containing 0.5 mL of DMPO (2 mmol). Electron spin resonance (ESR) signals of radicals spin-trapped by DMPO were recorded on a Bruker EMX 10/12 spectrometer with a TM110 cavity for emittance exchange. Typical ESR instrumental conditions were as follows: center field, 3475 G; sweep width, 200 G; resolution, 1024 pts; microwave frequency, ~9.79 GHz; modulation frequency, 100 kHz.

RESULTS AND DISCUSSION

Comparison of DO and PC. Crystal violet decomposition by DO and PC methods was monitored using UV/vis spectrophotometry. Based on preliminary experiments, the initial CV concentrations were set to ensure nearly complete degradation within 10 min for the DO and PC methods (100 and 50 mg/L, respectively). With either DO or PC, the intensity of the maximum absorption band of CV, initially at 584 nm, diminished substantially in 9 min (Figure 1), indicating both methods resulted in cleavage of the conjugated dye chromophore. Shifts in the absorption maxima occurred concomitantly with reduction in absorption intensity during the course of the reaction (Figure 1, insets). Interestingly, the shifts occurred in opposite directions for DO and PC, indicating different structural alterations of the CV structure. Considering the auxochromic property of the *N*-methyl group, the characteristic UV−vis absorption maximum of an intermediate with fewer *N*-methyl substituents than CV would be expected to shift to a shorter wavelength, which occurred with the PC process. The common hypsochromic shift from 584 to 576 nm likely resulted from the stepwise formation of *N*-demethylated intermediates during PC (Figure 1, upper panel), based on previous studies which showed that the dye Rhodamine B underwent a *N*-demethylation process when subjected to the PC method.[13,22,23] In contrast, a bathochromic shift from 584 to 592 nm was observed when DO was utilized (Figure 1, lower panel). This is a less common occurrence, though similar observations have been reported previously. For example, a bathochromic shift of 38 nm in UV−vis absorption spectrum of the crystal violet lactone was observed after 200 h of artificial daylight irradiation,[24] and Grocock et al.[25] reported that a 2-trifluoromethyl substitution on the CV molecule could lead to a bathochromic shift of 30 nm. In our experiments, the solution pH remained almost constant during and after the DO reaction hence the bathochromic shift associated with DO cannot be ascribed to a pH effect, further suggesting different degradation pathways for the DO and PC reactions. The work of Brooker et al.[26] suggests steric hindrance in CV can cause a bathochromic shift, and Dewar[27] has shown that the theoretical effect of an electron-withdrawing ortho-substituent on CV is a bathochromic shift in the UV−vis spectrum. The bathochromic shift manifested by the DO of CV in this study can plausibly be attributed to intermediates causing steric crowding, or the presence of electron-withdrawing substituents (see Discussion below).

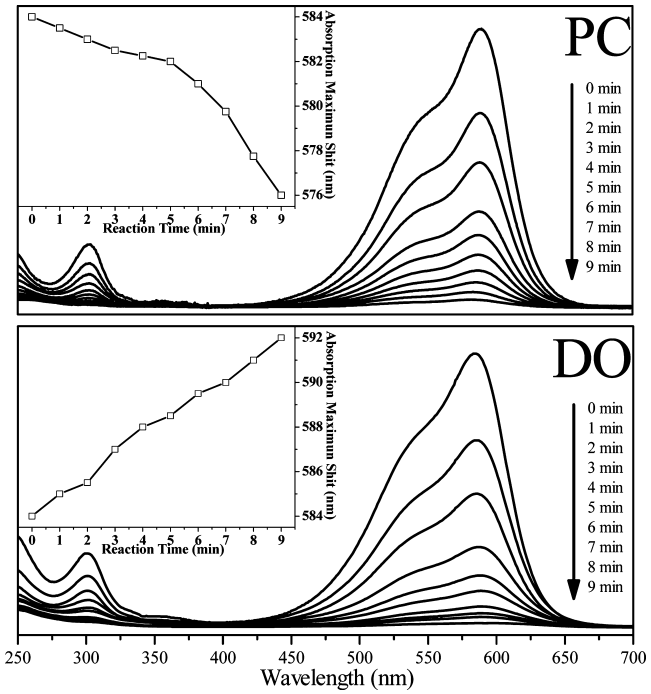

Figure 1. UV−vis spectra of crystal violet (CV) solution under different conditions: (upper panel) 100 mL of CV (50 mg/L) solution with 0.2 g of $NaBiO_3 \cdot 2H_2O$ in the visible light photocatalytic (PC) process and (lower panel) 100 mL of CV (100 mg/L) with bismuth silver oxide formed from 0.2 g of $NaBiO_3 \cdot 2H_2O$ in the direct oxidation (DO) process. Insets: wavelength shifts as a function of the decrease in absorption maximum.

Separation and Identification of the Intermediates. To further investigate the cause of opposite UV−vis spectral shifts associated with the PC and DO processes, LC/MS/MS and GC/MS were utilized to identify and monitor the formation of reaction intermediates.

LC/MS/MS Determination. LC/MS/MS was used to identify possible *N*-demethylated intermediates generated in the PC and DO process. In a typical ion chromatogram spectrum of the CV reaction solution formed in the PC reaction, the parent compound (CV, m/z = 372) and 10 other *N*-demethylated products were observed. These included an intermediate with one methyl group removed (m/z = 358), and nine intermediates with 2−5 fewer methyl groups than CV (m/z = 344, m/z = 330, m/z = 316, and m/z = 302 respectively) (Figure 2, left). These mass signals clearly indicate *N*-demethylation occurred during the PC process. In the reaction mixture from the DO process, however, among samples taken at different reaction times, only one *N*-demethylated intermediate was detected (Figure 2, right), indicating that *N*-demethylation was not a major CV degradation process during DO.

GC/MS Determination. There were 13 and 15 intermediates, mostly substituted benzenes and small molecular weight

dx.doi.org/10.1021/es3001954 | Environ. Sci. Technol. 2012, 46, 7318−7326

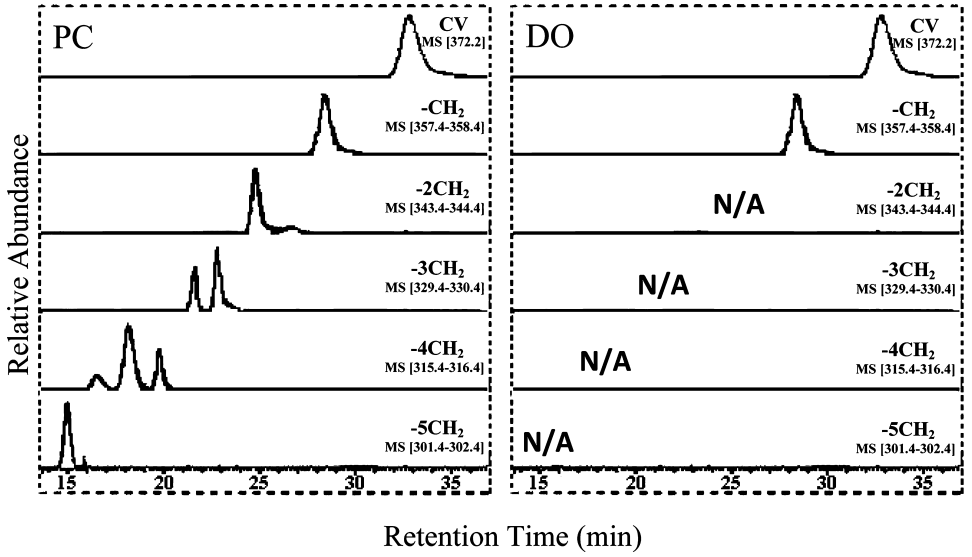

Figure 2. Typical LC/MS/MS chromatogram of the crystal violet solution in $NaBiO_3 \cdot 2H_2O$ initiated visible light photocatalytic (PC) process (left) and bismuth silver oxide initiated direct oxidation (DO) process (right). The *N*-demethylated products identified in PC process were indicated by signal m/z = 344, 330, 316, and 302, respectively, whereas only one *N*-demethylated product was identified in DO process.

alcohols, identified from the DO and PC process, respectively (NIST library with a fit value >70%) (Table S1). As suggested from the UV monitoring of reaction solutions, these degradation products indicate extensive cleavage of the CV chromophore structure. Eleven compounds were common to both the PC and DO process. Notably, the formation of intermediate P17 was determined in the reaction mixtures from both PC and DO, which results from cleavage at the central carbon.[28,29] Two degradation products (P5 and P13) were unique to the DO reaction and four (P8, P14−16) were unique to the PC reaction. It is apparent that significant differences exist in the CV degradation pathways for two reaction processes. For example, note the selective emergence of intermediate P13 in the DO process, and P15 in the PC process (Figure 3). The presence of intermediate P13, a major product from DO (Figure 3, upper panel), resulted from cleavage at the central carbon of CV, leaving the two methyl groups of the fragment intact. The formation of P13 suggests

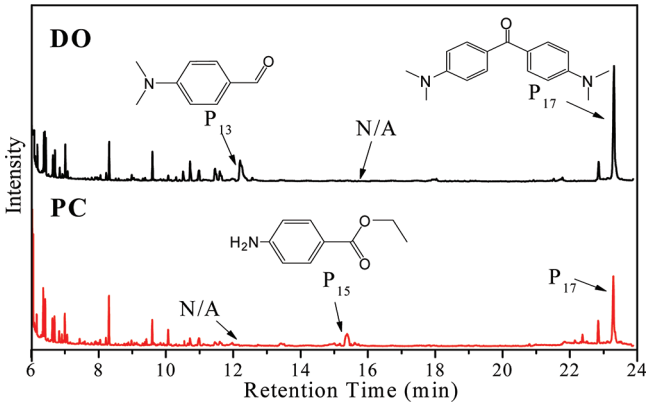

Figure 3. Typical GC/MS chromatogram obtained from an extract of crystal violet solution in bismuth silver oxide initiated direct oxidation (DO) process (upper panel) and in $NaBiO_3 \cdot 2H_2O$ initiated visible light photocatalytic (PC) process (lower panel). Selective emergence of intermediates P13, P15, and P17 is marked in both upper and lower panels.

that the *N*-methyl group of CV is not a major reactive center for the DO process. Extensive *N*-demethylation is characteristic of the PC process, and this accounts for the absence of P13 when this degradation process is employed (Figure 3, lower panel). One *N*-demethylated intermediate (i.e., P15) was unique to the PC process; no such *N*-demethylated product was detected in product mixtures emanating from the DO reaction, in good agreement with the LC/MS/MS result.

Mechanism. Based on results described above, some insights into the operative reaction mechanisms were apparent: Direct chromophore cleavage of CV is the predominant degradation pathway in the DO process, whereas in the PC process direct chromophore cleavage is accompanied by extensive *N*-demethylation. According to previous studies,[20,30] the dominant active oxygen species generated in the DO and PC reactions are $^1O_2$ and •OH radical, respectively. In the noncatalytic DO step, Bi(V) in BSO is progressively reduced as it oxidizes CV and is gradually transformed into $Bi_2O_2CO_3$ during which $^1O_2$ is generated from the lattice oxygen originally contained in the BSO perovskite structure. The difference in the dominant reactive oxygen species apparently manifests different CV degradation product profiles from DO vs PC processes. It is known that $^1O_2$ is more selective than •OH radical,[31] hence more reactive sites are available for •OH radical attack consistent with the greater number of CV degradation intermediates associated with the PC reaction.

The proposed CV degradation mechanism/pathway for the DO process is shown in Figure 4 (upper panel). Attack of $^1O_2$, generated from BSO, on the central phenyl-substituted C leads to the formation of a dioxeten intermediate, which decomposes further to give dimethylamino-benzophenones and dimethylaminophenol, and subsequently some small molecular weight intermediates such as intermediate P13.[24,32−34] One signal (m/z = 402) monitored by LC/MS/MS (data not shown) during the CV degradation via DO could plausibly be assigned to the dioxeten intermediate, which is generated from CV molecule (m/z = 372) by addition of two oxygen atoms with concomitant abstraction of two hydrogen atoms. Previous calculation on the π-electron density of CV using Pariser−

dx.doi.org/10.1021/es3001954 | Environ. Sci. Technol. 2012, 46, 7318−7326

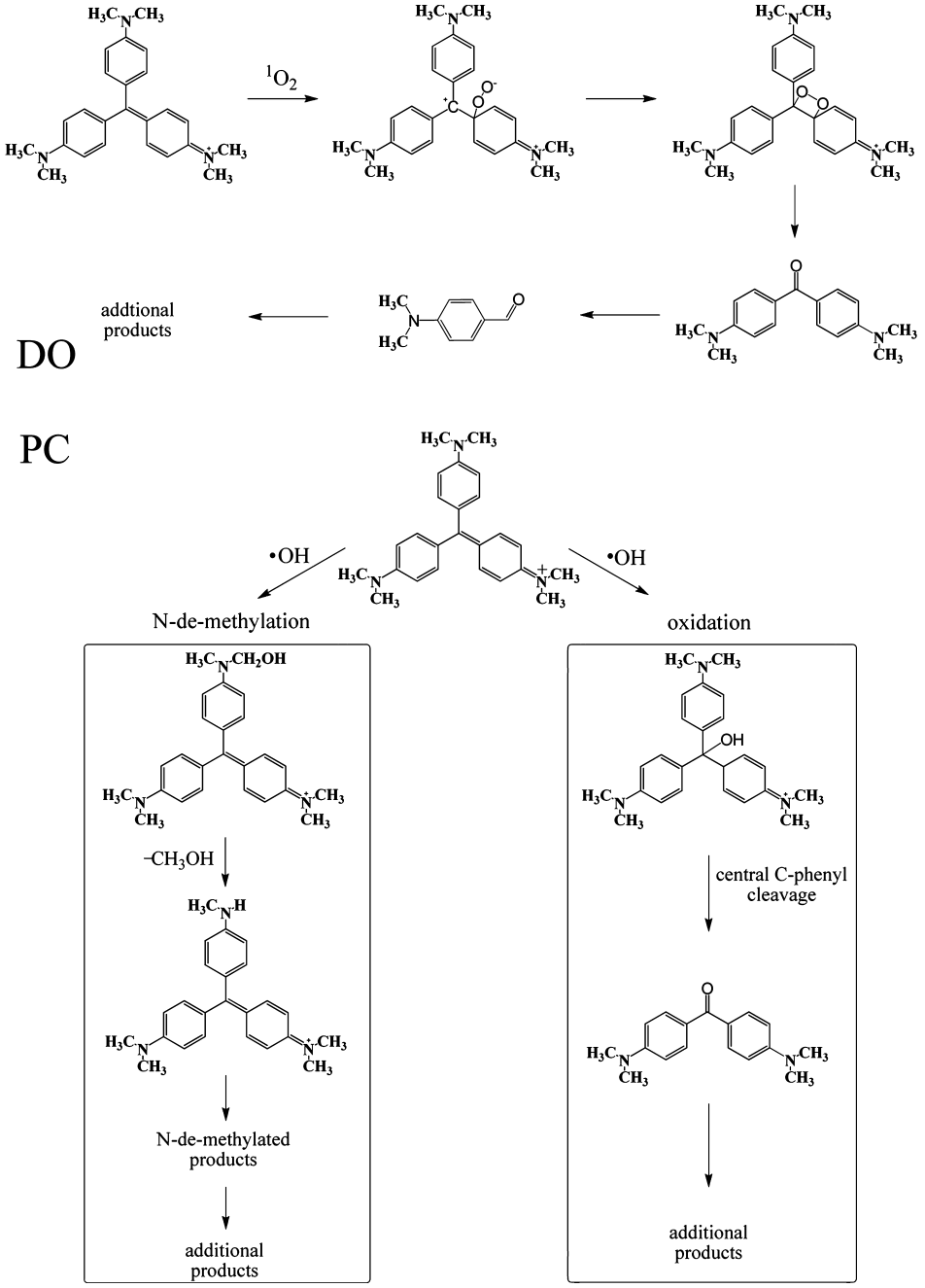

Figure 4. Proposed schematic crystal violet (CV) degradation pathway in bismuth silver oxide initiated direct oxidation (DO) process (shown in upper panel: attack of $^1O_2$, on the central phenyl substituted C leads to the formation of a dioxeten intermediate, which decomposes further to give some small molecular weight intermediates; no significant *N*-demethylation was observed) and $NaBiO{\cdot}2H_2O$ initiated visible light photocatalytic (PC) process (shown in lower panel: degradation pathway of CV includes two parts, viz. *N*-demethylation, which occurred via •OH radical attack on the *N*-methyl groups of CV parent molecule and partially *N*-demethylated intermediates, and chromophore cleavage, which occurred via •OH radical attack on the central phenyl-substituted carbon, yielding various aromatic derivatives and benzene ring-cleavage products).

Parr−Pople molecular orbital calculation method supports the emergence of this species.[32] Interestingly, the nonbonded electrons in the oxo-bridge over the central carbon could conjugate with the π-system of the dye chromophore hence presenting some auxochrome effect; this might explain the increasing maximum absorption wavelength observed by UV/vis spectrophotometry.

Due to the relatively nonselective reactivity of •OH radicals,[31,35] the degradation pathway of CV via the PC reaction includes two parts, viz. *N*-demethylation and chromophore cleavage (Figure 4, lower panel).[21,36−38] The *N*-demethylation occurs via •OH radical attack on the *N*-methyl groups of the CV parent molecule and partially *N*-demethylated intermediates, resulting in the formation of completely *N*-demethylated intermediates such as P15.[28,39] The chromophore of CV is attacked by •OH species on the central phenyl-substituted carbon, which subsequently yields various aromatic derivatives and benzene ring-cleavage products, and ultimately complete mineralization.[40]

Decolorization Performance. The decolorizing ability of DO and PC methods was compared by mixing 100 mL of aqueous CV solutions at concentrations of 30, 60, 100, 150, and

dx.doi.org/10.1021/es3001954 | Environ. Sci. Technol. 2012, 46, 7318−7326

200 mg/L with BSO (prepared using 0.2 g of $NaBiO_3 \cdot 2H_2O$) as the oxidant for the DO process, and 0.2 g of $NaBiO_3 \cdot 2H_2O$ as the photocatalyst for the PC process. The initial CV reaction rates were higher for DO compared to PC (Figure 5, inserts),

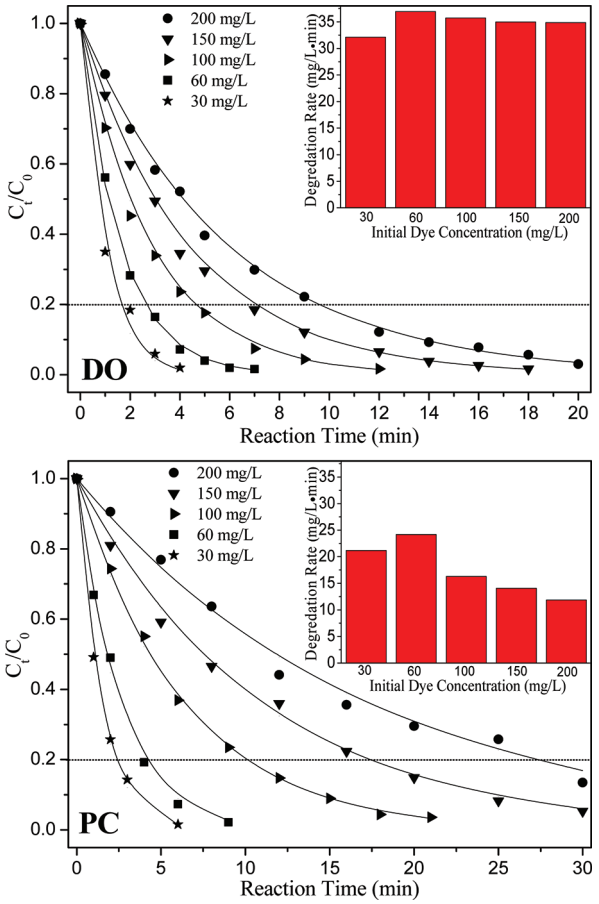

Figure 5. Relative concentration decrease (C_t/C_0) for various initial concentrations of crystal violet (CV) in solution at time zero (C_0) and at increasing reaction times (C_t) in the direct oxidation (DO) process (upper panel) and visible light photocatalytic (PC) process (lower panel). Inserts: initial degradation rates manifested by different initial concentrations of dye. Experimental conditions: 100 mL of CV solution with concentrations at 30, 60, 100, 150, and 200 mg/L, respectively; bismuth silver oxide formed from 0.2 g of $NaBiO_3 \cdot 2H_2O$ used in DO process and 0.2 g of $NaBiO_3 \cdot 2H_2O$ used in PC process.

and for both DO and PC processes that degradation rate increased when the initial CV concentration increased from 30 to 60 mg/L; any further increase in CV concentration (100–200 mg/L) led to a slight decrease in the DO reaction rates, whereas the PC reaction rates declined significantly.

It is known that radical initiation in heterogeneous catalytic/oxidative degradation reactions requires reactant adsorption on the particle surface and then formation of active radicals (ARs).[41] The initial reaction rate R can be expressed by eq 1

$$R = k_0 \bullet P_{ARs} \bullet P_{dye} \bullet [\text{Dye}] \quad (1)$$

where k_0 is the unit reaction rate constant, P_{ARs} is the probability of generating active radicals on the particle surface, P_{dye} is the probability of surface adsorbed CV dye molecules reacting with the active oxygen radicals, and [Dye] is the initial CV dye concentration. The rate constant k_0 is independent of the initial dye concentration, but P_{ARs} and P_{dye} depend implicitly on the dye concentration. As the initial dye concentration increases the probability of reaction between dye molecules and the oxidizing species is expected, a priori, to increase, leading to an enhancement in the decolorization rate for both DO and PC processes. In our experiments, as the initial CV concentration exceeded 60 mg/L the rate either plateaued or decreased in the DO and PC processes, respectively. Because the quantity of BSO was fixed in the DO processes, it is reasonable to assume the rate and amount of $^1O_2$ released was constant, based on our previous study.[20] Hence, as the CV concentration increased, the quantity of BSO became rate limiting, and the reaction rate essentially plateaued. For the PC processes, the generation of active oxygen requires external light-induced excitement at the surface of photocatalyst. Increasing the concentration of CV results in more dye ion coverage on the surface active sites of $NaBiO_3 \cdot 2H_2O$ where •OH is formed. More importantly, because of the strong absorbance of visible light by CV, the progressive increase in CV concentration inhibited light penetration and illumination at the photocatalyst surface, thereby reducing production of •OH, and in turn the reaction rate, as observed.

To further investigate the effect of dye concentration on degradation reaction, electron spin-trapping (ESR) technique was utilized to determine the radicals involved in the reaction processes. The ESR signal of DMPO–$^1O_2$ with characteristic three longer and four shorter lines,[20,42] and DMPO–•OH with four characteristic lines with an intensity ratio of 1:2:2:1[43,44] confirmed the generation of $^1O_2$ and •OH radicals in DO and PC, respectively (Figure S2). It is evident that the generation of $^1O_2$ was mostly independent of the CV concentration in DO reaction solution (Figure S2 a), whereas the signal intensity of DMPO–•OH decreased as the CV concentration increased from 30 to 200 mg/L, indicating the generation of •OH was in inverse ratio to CV concentration as expected (Figure S2 b). Thus, according to eq 1, at higher dye concentration the PC reaction rate slowed due to reduced generation of •OH which lowers the probability factor P_{ARs}, whereas the DO rate remains nearly constant in DO as the dye concentration increased. As a result, the PC process took more time than the DO process to achieve the same extent of decolorization. For instance, achieving 80% decolorization of CV by the DO treatment process required 1.6, 2.7, 4.6, 7.1, and 9.6 min at initial CV solutions of 30, 60, 100, 150, and 200 mg/L, respectively; the corresponding time required by the PC treatment process was 2.8, 4.6, 10.1, 17.4, and 27.1 min, respectively (Figure 5). This demonstrates that with respect to decolorization, the DO process is more favorable than the PC process, especially for high concentrations of dye in wastewater.

Combined Processes. It has been widely reported that some degradation intermediates are more toxic and carcinogenic than the parent compounds.[3,45] Hence, the complete mineralization of dye components prior to wastewater discharging is highly desirable. The TOC is also a common water quality criterion, and its reduction is favorable. Our results (Figure 6) showed that TOC removal efficiency by the DO process plateaued eventually. This could be ascribed to more selectivity and less oxidative ability of $^1O_2$ generated in the DO process.[46] In this regard, the DO process has not maximized the quality of the simulated treated dye wastewater (i.e., CV solution), in terms of TOC, and in practice this could result in failure to satisfy discharge standards. Although the •OH radicals generated in the PC process promote the degradation of a wide range of contaminants efficiently,[2] dye

dx.doi.org/10.1021/es3001954 | Environ. Sci. Technol. 2012, 46, 7318–7326

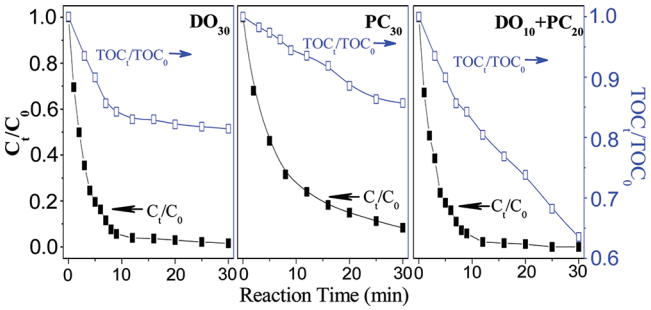

Figure 6. Relative concentration decrease (C_t/C_0) and relative mineralization degree (TOC_t/TOC_0) of 100 mL of crystal violet (CV) solution (130 mg/L) as a function of reaction time under different degradation conditions: separately utilized 30 min of direct oxidation (DO) process (left panel), separately utilized 30 min of visible light photocatalytic (PC) process (middle panel), and the sequential use of DO (10 min) and then PC (20 min) processes (right panel). Experimental conditions: bismuth silver oxide formed from 0.2 g of $NaBiO_3{\cdot}2H_2O$ used in DO process and 0.2 g of $NaBiO_3{\cdot}2H_2O$ used in PC process; same condition in separate and combined processes. Relative concentration decrease (C_t/C_0) and contents (TOC_t/TOC_0) are calculated using initial CV concentration (C_0) and initial total organic carbon (TOC) content (TOC_0), and CV concentration (C_t) and TOC content (TOC_t) at increasing reaction time.

degradation via the PC process would be significantly inhibited by the light-filtering effects of the colored dye solution.

Considering the incomplete degradation/mineralization achieved by the DO and PC processes individually, the efficiency of treating a CV solution (130 mg/L) by the sequential use of DO (10 min) and then PC (20 min) processes was conducted to investigate the combined effect on TOC and color removal performance. The two comparison experiments (DO alone and PC alone) were carried out under otherwise identical conditions. More than 95% decolorization of the dye was achieved in 10 min using the DO process alone, whereas the PC process required more than 30 min to reach the same degree of decolorization (Figure 6). Deep mineralization was not observed in the DO process; TOC removal stopped at about 18% after the solution was completely bleached. Approximately 15% of the TOC removal was achieved in 30 min via the PC reaction alone. Although this is slightly less than that achieved via the DO reaction over the same time range, the TOC removal did not plateau, suggesting that with time additional mineralization could be achieved. This contention is theoretically supported by the higher oxidation potential of •OH radical (2.8 eV), such that the PC reaction has the potential to achieve extensive mineralization of CV and similar dyes. In the combined experiment, a total 37% TOC removal was achieved in 30 min, which represents a >100% increase in TOC removal compared to that achieved employing the DO or PC process separately (Figure 6). Notably, in the combined process, TOC removal proceeds in a linear fashion and at a much higher rate than that achieved by DO or PC, indicating that extensive TOC removal is plausible. Furthermore, in the combined process about 20% TOC removal was achieved in 20 min whereas only 15% TOC removal was achieved in the individually employed 30 min-PC process, hence suggesting benefits derived from a synergistic effect when DO is used with PC.

The practical application of the treatment approach based on coupled DO and PC processes would be strengthened if it had the capability of treating a wide range of organic dyes. To evaluate the versatility of the combined sequential DO−PC processes, high concentrations of different dyes, i.e. 500 mg/L of safranin T (safranin), 200 mg/L of azure B (thiazin), 150 mg/L of malachite green (triarylmethane), 75 mg/L of crystal violet (triarylmethane), and 250 mg/L of alizarin red (anthraquinone) were chosen for treatment. The DO and PC processes were utilized alone and in combination; for each dye the same total treatment times (for DO, PC, and DO plus PC) and experimental conditions were employed. Reaction times for each process were optimized (minimal DO treatment time for decolorization) for different dyes in the preliminary experiments with the following results: 13 min of DO then 47 min of PC for safranin T; 10 min of DO then 40 min of PC for azure B; 5 min of DO then 25 min of PC for malachite green; 3 min of DO then 17 min of PC for crystal violet; 15 min of DO then 45 min of PC for alizarin red. The combined process manifested dramatically improved mineralization of this diverse groups of dyes compared to that achieved using DO or PC processes alone for the same total treatment time (Figure S3), as documented for CV. Significant mineralization (~35 to 45%) was achieved for each dye demonstrating the broad application of this technology for treating aqueous dye solutions. In addition, our previous results indicated that $NaBiO_3$ was highly stable during five repeated rhodamine B (a dye similar to CV) degradation processes,[13] and BSO was not substantially fouled during 16 sequential rhodamine B degradation cycles;[20] these previous experiments were conducted under conditions identical to those in the present experiment.

The TOC removed in the combined process is the sum of TOC removed during the DO stage and PC stages, in sequence. Based on results obtained when using DO alone (Figure 6), TOC removal by DO in the combined process occurred primarily during the early decolorizing stage, which also eliminates the light filtering effect of the original deeply colored solution. The TOC removal during the PC stage of the combined method should exceed TOC removal when PC alone is utilized. The highly transparent effluent from the DO stage of the combined process allows more photos to reach the photocatalyst by reducing light adsorption by the dye molecules. This results in a larger degree of light-generated hole/electron pair excitation, leading to the generation of more •OH radicals, and in turn, greater pollutant mineralization. Also, $^1O_2$ formed by DO may facilitate PC performance in another way. In the isolated PC process, •OH radicals function in three ways: *N*-demethylation, decolorization, or mineralization, i.e., attack of the *N*-methyl groups, the central phenyl substituted C, or the benzene ring structure. Considering the electrophilic nature of •OH radicals,[47] initial attack should occur preferentially at the most electron-rich sites in CV, namely the *N*-methyl groups and the central phenyl substituted C. Consequently, if limited in quantity, fewer •OH radicals would be available for benzene ring-opening and hence TOC removal. However, in the combined process, cleavage of the CV dye chromophore during the DO stage, and the resultant disappearance of the planar resonance structure renders the *N*-methyl groups and central carbon less electron-rich. As a result, hydroxyl radicals generated in the sequential PC process are more likely to attack benzene compounds, eventually leading to mineralization. Considering that the decolorizing reaction occurs relatively fast during the DO stage of the combined process, the subsequent PC process has almost the same

dx.doi.org/10.1021/es3001954 | Environ. Sci. Technol. 2012, 46, 7318−7326

(though slightly reduced) time remaining for TOC removal, when considering fixed units of treatment time.

In summary, the proposed technology is based on utilizing two $NaBiO_3$-based materials in sequence to initiate two separate processes, which together extensively degrade a wide variety of organic dyes in water. First DO performs a bleaching function accompanied by TOC removal that occurs rapidly but plateaued. The subsequent PC process exhibits improved levels of decomposition and mineralization. The PC function is improved due to increased light penetration, and because reactivity is directed toward intermediates (from DO) leading to efficient mineralization and TOC reduction. This is the first report directly comparing two $NaBiO_3$ based materials aimed at treating dye contaminated wastewaters, and demonstrates benefits accrued by their use in sequence. Each produces distinct primary active oxygen species, i.e. BSO generated $^1O_2$ in the DO process, and $NaBiO_3 \cdot 2H_2O$ generated •OH in the PC process, manifesting different CV dye degradation pathways. The results presented here document for the first time that vastly improved mineralization was achieved during a fixed unit of treatment time by utilizing DO and PC processes in sequence compared to either treatment method used singularly. These results provide the basis of a new approach for the rapid decolorization and mineralization of dyes present in highly contaminated wastewater which utilizes visible light, and is operationally simple.

■ ASSOCIATED CONTENT

Supporting Information

Additional table and figures (Table S1. Comparison of CV degradation intermediates identified by GC/MS in DO and PC reaction processes, respectively. Figure S1. Chemical Structure of CV. Figure S2. Effect of CV concentration on the intensity of the DMPO−$^1O_2$ and DMPO−•OH adduct ESR signal in the DO and PC processes, respectively. Figure S3. Mineralization comparison of three different methods (separately utilized DO process, separately utilized PC process, and sequentially utilized DO and PC processes) on treating 100 mL different high concentrations of organic dye solution over the same total reaction time). This material is available free of charge via the Internet at http://pubs.acs.org.

■ AUTHOR INFORMATION

Corresponding Author

*Tel: +86-25-89680258; fax: +86-25-89680580; e-mail: envidean@nju.edu.cn (C.S.); Tel: (517) 355-0271 ext. 252; fax: (517) 355-0270; e-mail: boyds@msu.edu (S.B.).

Notes

The authors declare no competing financial interest.

■ ACKNOWLEDGMENTS

This work was supported by the National Natural Science Foundation of China (21177055 and 20737001) and Natural Science Foundation of Jiangsu Province (BK2009254).

■ REFERENCES

(1) Vanhulle, S.; Trovaslet, M.; Enaud, E.; Lucas, M.; Taghavi, S.; Van Der Lelie, D.; Van Aken, B.; Foret, M.; Onderwater, R. C. A.; Wesenberg, D.; Agathos, S. N.; Schneider, Y. J.; Corbisier, A. M. Decolorization, cytotoxicity, and genotoxicity reduction during a combined ozonation/fungal treatment of dye-contaminated wastewater. *Environ. Sci. Technol.* **2008**, *42* (2), 584−589.

(2) Guelli Ulson de Souza, S. M. d. A.; Santos Bonilla, K. A.; Ulson de Souza, A. A. Removal of COD and color from hydrolyzed textile azo dye by combined ozonation and biological treatment. *J. Hazard. Mater.* **2010**, *179* (1−3), 35−42.

(3) Berberidou, C.; Avlonitis, S.; Poulios, I. Dyestuff effluent treatment by integrated sequential photocatalytic oxidation and membrane filtration. *Desalination* **2009**, *249* (3), 1099−1106.

(4) Ohko, Y.; Ando, I.; Niwa, C.; Tatsuma, T.; Yamamura, T.; Nakashima, T.; Kubota, Y.; Fujishima, A. Degradation of bisphenol A in water by TiO_2 photocatalyst. *Environ. Sci. Technol.* **2001**, *35* (11), 2365−2368.

(5) Malato, S.; Blanco, J.; Vidal, A.; Richter, C. Photocatalysis with solar energy at a pilot-plant scale: An overview. *Appl. Catal., B* **2002**, *37* (1), 1−15.

(6) Selli, E. Synergistic effects of sonolysis combined with photocatalysis in the degradation of an azo dye. *Phys. Chem. Chem. Phys.* **2002**, *4* (24), 6123−6128.

(7) Zhang, Z. H.; Yuan, Y.; Liang, L. H.; Fang, Y. J.; Cheng, Y. X.; Ding, H. C.; Shi, G. Y.; Jin, L. T. Sonophotoelectrocatalytic degradation of azo dye on TiO_2 nanotube electrode. *Ultrason. Sonochem.* **2008**, *15* (4), 370−375.

(8) Stock, N. L.; Peller, J.; Vinodgopal, K.; Kamat, P. V. Combinative sonolysis and photocatalysis for textile dye degradation. *Environ. Sci. Technol.* **2000**, *34* (9), 1747−1750.

(9) Kim, J.; Lee, C. W.; Choi, W. Platinized WO_3 as an environmental photocatalyst that generates OH radicals under visible light. *Environ. Sci. Technol.* **2010**, *44* (17), 6849−6854.

(10) Liao, G. Z.; Chen, S.; Quan, X.; Chen, H.; Zhang, Y. B. Photonic crystal coupled TiO_2/polymer hybrid for efficient photocatalysis under visible light irradiation. *Environ. Sci. Technol.* **2010**, *44* (9), 3481−3485.

(11) Li, Y. Y.; Yao, S. S.; Wen, W.; Xue, L. H.; Yan, Y. W. Sol-gel combustion synthesis and visible-light-driven photocatalytic property of perovskite $LaNiO_3$. *J. Alloys Compd.* **2010**, *491* (1−2), 560−564.

(12) Sulaeman, U.; Yin, S.; Sato, T. Visible light photocatalytic activity induced by the carboxyl group chemically bonded on the surface of $SrTiO_3$. *Appl. Catal., B* **2011**, *102* (1−2), 286−290.

(13) Yu, K.; Yang, S. G.; He, H.; Sun, C.; Gu, C. G.; Ju, Y. M. Visible light-driven photocatalytic degradation of rhodamine B over $NaBiO_3$: Pathways and mechanism. *J. Phys. Chem. A* **2009**, *113* (37), 10024−10032.

(14) Chang, X. F.; Huang, J.; Cheng, C.; Sha, W.; Li, X.; Ji, G. B.; Deng, S. B.; Yu, G. Photocatalytic decomposition of 4-t-octylphenol over $NaBiO_3$ driven by visible light: Catalytic kinetics and corrosion products characterization. *J. Hazard. Mater.* **2010**, *173* (1−3), 765−772.

(15) Kou, J. H.; Zhang, H. T.; Li, Z. S.; Ouyang, S. X.; Ye, J. H.; Zou, Z. G. Photooxidation of polycyclic aromatic hydrocarbons over $NaBiO_3$ under visible light irradiation. *Catal. Lett.* **2008**, *122* (1−2), 131−137.

(16) Kako, T.; Zou, Z. G.; Katagiri, M.; Ye, J. H. Decomposition of organic compounds over $NaBiO_3$ under visible light irradiation. *Chem. Mater.* **2007**, *19* (2), 198−202.

(17) Chang, X. F.; Huang, J.; Cheng, C.; Sha, W.; Li, X.; Ji, G. B.; Deng, S. B.; Yu, G. Photocatalytic decomposition of 4-t-octylphenol over $NaBiO_3$ driven by visible light: Catalytic kinetics and corrosion products characterization. *J. Hazard. Mater.* **2010**, *173* (1−3), 765−772.

(18) Teraoka, Y.; Kanada, K.; Kagawa, S. Synthesis of La-K-Mn-O perovskite-type oxides and their catalytic property for simultaneous removal of NO_x and diesel soot particulates. *Appl. Catal., B* **2001**, *34* (1), 73−78.

(19) Bialobok, B.; Trawczynski, J.; Rzadki, T.; Mista, W.; Zawadzki, M. Catalytic combustion of soot over alkali doped $SrTiO_3$. *Catal. Today* **2007**, *119* (1−4), 278−285.

(20) Yu, K.; Yang, S. G.; Boyd, S. A.; Chen, H. Z.; Sun, C. Efficient degradation of organic dyes by $BiAg_xO_y$. *J. Hazard. Mater.* **2011**, *197*, 88−96.

(21) Chen, C. C.; Chen, W. C.; Chiou, M. R.; Chen, S. W.; Chen, Y. Y.; Fan, H. J. Degradation of crystal violet by an FeGAC/H_2O_2 process. *J. Hazard. Mater.* **2011**, *196*, 420−425.
(22) Yin, M. C.; Li, Z. S.; Kou, J. H.; Zou, Z. G. Mechanism investigation of visible light-induced degradation in a heterogeneous TiO_2/Eosin Y/rhodamine B system. *Environ. Sci. Technol.* **2009**, *43* (21), 8361−8366.
(23) Fu, H. B.; Zhang, S. C.; Xu, T. G.; Zhu, Y. F.; Chen, J. M. Photocatalytic degradation of RhB by fluorinated Bi_2WO_6 and distributions of the intermediate products. *Environ. Sci. Technol.* **2008**, *42* (6), 2085−2091.
(24) Caine, M. A.; McCabe, R. W.; Wang, L. C.; Brown, R. G.; Hepworth, J. D. The influence of singlet oxygen in the fading of carbonless copy paper primary dyes on clays. *Dyes Pigm.* **2001**, *49* (3), 135−143.
(25) Grocock, D. E.; Hallas, G.; Hepworth, J. D. Steric effects in di-Arylmethane and tri-Arylmethane dyes 0.11. electronic absorption-spectra of derivatives of michlers hydrol blue, crystal violet, and malachite green containing ortho-trifluoromethyl groups. *J. Chem. Soc. Perkins Trans. 2* **1973**, No. 13, 1792−1796.
(26) Brooker, L. G. S.; White, F. L.; Sprague, R. H.; Dent, S. G.; Van Zandt, G. Steric hindrance to planarity in dye molecules. *Chem. Rev.* **1947**, *41* (2), 325−351.
(27) Dewar, M. J. S. Colour and constitution. Part I. Basic dyes. *J. Chem. Soc.* **1950**, 2329−2334.
(28) Fan, H. J.; Huang, S. T.; Chung, W. H.; Jan, J. L.; Lin, W. Y.; Chen, C. C. Degradation pathways of crystal violet by Fenton and Fenton-like systems: Condition optimization and intermediate separation and identification. *J. Hazard. Mater.* **2009**, *171* (1−3), 1032−1044.
(29) Mai, F. D.; Chen, C. C.; Chen, J. L.; Liu, S. C. Photodegradation of methyl green using visible irradiation in ZnO suspensions: Determination of the reaction pathway and identification of intermediates by a high-performance liquid chromatography-photo-diode array-electrospray ionization-mass spectrometry method. *J. Chromatogr., A* **2008**, *1189* (1−2), 355−365.
(30) Chang, X. F.; Ji, G. B.; Sui, Q.; Huang, J.; Yu, G. Rapid photocatalytic degradation of PCP-Na over $NaBiO_3$ driven by visible light irradiation. *J. Hazard. Mater.* **2009**, *166* (2−3), 728−733.
(31) Foote, C. S.; Shook, F. C.; Abakerli, R. B. Characterization of singlet oxygen. *Methods Enzymol.* **1984**, *105*, 36−47.
(32) Kuramoto, N.; Kitao, T. The contribution of singlet oxygen to the photofading of triphenylmethane and related dyes. *Dyes Pigm.* **1982**, *3* (1), 49−58.
(33) Kuramoto, N.; Kitao, T. Contribution of singlet oxygen to the photofading of some dyes. *J. Soc. Dyers Colour.* **1982**, *98* (10), 334−340.
(34) Weyermann, C.; Kirsch, D.; Vera, C. C.; Spengler, B. Evaluation of the photodegradation of crystal violet upon light exposure by mass spectrometric and spectroscopic methods. *J. Forensic Sci.* **2009**, *54* (2), 339−345.
(35) Lee, Y.; von Gunten, U. Oxidative transformation of micropollutants during municipal wastewater treatment: Comparison of kinetic aspects of selective (chlorine, chlorine dioxide, ferrate(VI), and ozone) and non-selective oxidants (hydroxyl radical). *Water Res.* **2010**, *44* (2), 555−566.
(36) Fan, H. J.; Lu, C. S.; Lee, W. L. W.; Chiou, M. R.; Chen, C. C. Mechanistic pathways differences between P25-TiO_2 and Pt-TiO_2 mediated CV photodegradation. *J. Hazard. Mater.* **2011**, *185*, 227−235.
(37) Mai, F. D.; Lee, W. L. W.; Chang, J. L.; Liu, S. C.; Wu, C. W.; Chen., C. C. Fabrication of porous TiO_2 film on Ti foil by hydrothermal process and its photocatalytic efficiency and mechanisms with ethyl violet dye. *J. Hazard. Mater.* **2010**, *177*, 864−875.
(38) Liao, Y. H. B.; Wang, J. X.; Lin, J. S.; Chung, W. H.; Lin, W. Y.; Chen, C. C. Synthesis, photocatalytic activities and degradation mechanism of Bi_2WO_6 toward crystal violet dye. *Catal. Today* **2011**, *174*, 148−159.
(39) Chen, C. C.; Mai, F. D.; Chen, K. T.; Wu, C. W.; Lu, C. S. Photocatalyzed N-de-methylation and degradation of crystal violet in titania dispersions under UV irradiation. *Dyes Pigm.* **2007**, *75* (2), 434−442.
(40) Gupta, A. K.; Pal, A.; Sahoo, C. Photocatalytic degradation of a mixture of Crystal Violet (Basic Violet 3) and Methyl Red dye in aqueous suspensions using Ag+ doped TiO_2. *Dyes Pigm.* **2006**, *69* (3), 224−232.
(41) Sakthivel, S.; Neppolian, B.; Shankar, M. V.; Arabindoo, B.; Palanichamy, M.; Murugesan, V. Solar photocatalytic degradation of azo dye: Comparison of photocatalytic efficiency of ZnO and TiO_2. *Sol. Energy Mater. Sol. Cells* **2003**, *77*, 65−82.
(42) Ben-Hur, E.; Carmichael, A.; Riesz, P.; Rosenthal, I. Photo-chemical generation of superoxide radical and the cytotoxicity of phthalocyanines. *Int. J. Radiat. Biol.* **1985**, *48* (5), 837−846.
(43) Wang, Z. H.; Chen, X.; Ji, H. W.; Ma, W. H.; Chen, C. C.; Zhao, J. C. Photochemical cycling of iron mediated by dicarboxylates: Special effect of malonate. *Environ. Sci. Technol.* **2010**, *44* (1), 263−268.
(44) Wu, T. X.; Lin, T.; Zhao, J. C.; Hidaka, H.; Serpone, N. TiO_2-assisted photodegradation of dyes. 9. Photooxidation of a squarylium cyanine dye in aqueous dispersions under visible light irradiation. *Environ. Sci. Technol.* **1999**, *33* (9), 1379−1387.
(45) Jakopitsch, C.; Regelsberger, G.; Furtmuller, P. G.; Ruker, F.; Peschek, G. A.; Obinger, C. Catalase-peroxidase from Synechocystis is capable of chlorination and bromination reactions. *Biochem. Biophys. Res. Commun.* **2001**, *287* (3), 682−687.
(46) Koppenol, W. H.; Stanbury, D. M.; Bounds, P. L. Electrode potentials of partially reduced oxygen species, from dioxygen to water. *Free Radical Biol. Med.* **2010**, *49* (3), 317−322.
(47) Chen, C. C.; Lu, C. S. Mechanistic studies of the photocatalytic degradation of methyl green: An investigation of products of the decomposition processes. *Environ. Sci. Technol.* **2007**, *41* (12), 4389−4396.